



# Cyclic Adenosine Monophosphate (cAMP)-Dependent Phosphodiesterase Inhibition Promotes Bone Anabolism Through CD8<sup>+</sup> T Cell Wnt-10b Production in Mice

Susanne Roser-Page,<sup>1</sup> Daiana Weiss,<sup>2</sup> Tatyana Vikulina,<sup>1,2</sup> Mingcan Yu,<sup>2</sup> Roberto Pacifici,<sup>2</sup>  and M. Neale Weitzmann<sup>1,2</sup> 

<sup>1</sup>Atlanta Department of Veterans Affairs Medical Center, Decatur, GA, USA

<sup>2</sup>Division of Endocrinology and Metabolism and Lipids, Department of Medicine, Emory University School of Medicine, Atlanta, GA, USA

## ABSTRACT

Cyclic adenosine monophosphate (cAMP)-dependent phosphodiesterase (PDE) inhibitors such as pentoxifylline (PTX) suppress cAMP degradation and promote cAMP-dependent signal transduction. PDE inhibitors increase bone formation and bone mass in preclinical models and are used clinically to treat psoriatic arthritis by targeting inflammatory mediators including activated T cells. T cell activation requires two signals: antigen-dependent CD3-activation, which stimulates cAMP production; and CD28 co-stimulation, which downregulates cAMP-signaling, through PDE activation. PDE-inhibitors consequently suppress T cell activation by disrupting CD28 co-stimulation. Interestingly, we have reported that when CD8<sup>+</sup> T cells are activated in the absence of CD28 co-stimulation, they secrete Wnt-10b, a bone anabolic Wnt ligand that promotes bone formation. In the present study, we investigated whether the bone anabolic activity of the PDE-inhibitor PTX, has an immunocentric basis, involving Wnt-10b production by CD8<sup>+</sup> T cells. When wild-type (WT) mice were administered PTX, biochemical markers of both bone resorption and formation were significantly increased, with net bone gain in the axial skeleton, as quantified by micro-computed tomography ( $\mu$ CT). By contrast, PTX increased only bone resorption in T cell knockout (KO) mice, causing net bone loss. Reconstituting T cell-deficient mice with WT, but not Wnt-10b knockout (KO) CD8<sup>+</sup> T cells, rescued bone formation and prevented bone loss. To study the role of cAMP signaling in Wnt-10b expression, reverse-transcription polymerase chain reaction (RT-PCR) and luciferase-reporter assays were performed using primary T cells. PDE inhibitors intensified Wnt-10b promoter activity and messenger RNA (mRNA) accumulation in CD3 and CD28 activated CD8<sup>+</sup> T cells. In contrast, inhibiting the cAMP pathway mediators protein kinase A (PKA) and cAMP response element-binding protein (CREB), suppressed Wnt-10b expression by T cells activated in the absence of CD28 co-stimulation. In conclusion, the data demonstrate a key role for Wnt-10b production by CD8<sup>+</sup> T cells in the bone anabolic response to PDE-inhibitors and reveal competing T cell-independent pro-resorptive properties of PTX, which dominate under T cell-deficient conditions. Selective targeting of CD8<sup>+</sup> T cells by PDE inhibitors may be a beneficial approach for promoting bone regeneration in osteoporotic conditions. © 2022 The Authors. *JBMR Plus* published by Wiley Periodicals LLC on behalf of American Society for Bone and Mineral Research.

**KEY WORDS:** ANABOLICS; THERAPEUTICS; OSTEOBLASTS; CELLS OF BONE; OSTEOIMMUNOLOGY; SYSTEMS BIOLOGY-BONE INTERACTORS

## Introduction

The immunoskeletal interface is a nexus between immune and skeletal systems, resulting from the repurposing of immune cells and their cytokine mediators, for skeletal functions.<sup>(1)</sup> As a consequence, inflammation and other immunological perturbations have the potential to drive bone loss in multiple conditions including rheumatoid arthritis, periodontitis, Crohn's disease, estrogen deficiency, hyperparathyroidism, human immunodeficiency virus (HIV) infection, and immune

reconstitution following antiretroviral therapy against HIV.<sup>(1,2)</sup> In these states, bone loss is driven by osteoclastogenic factors including receptor activator of nuclear factor  $\kappa$ B ligand (RANKL), tumor necrosis factor  $\alpha$  (TNF $\alpha$ ), interferon  $\gamma$  (IFN $\gamma$ ), and interleukin (IL)-17A, secreted by activated adaptive immune cells including CD4<sup>+</sup> and CD8<sup>+</sup> T cells, B cells, and macrophages.<sup>(1-6)</sup>

Interestingly, anti-osteoclastogenic roles of CD8<sup>+</sup> T cells have also been recognized, although until recently, the mechanisms of action could not be determined.<sup>(7,8)</sup> Intriguingly, studies now reveal that exposure of CD8<sup>+</sup> T cells to low-dose RANKL can

This is an open access article under the terms of the [Creative Commons Attribution](#) License, which permits use, distribution and reproduction in any medium, provided the original work is properly cited.

Received in original form February 25, 2022; revised form April 22, 2022; accepted May 5, 2022.

Address correspondence to: M. Neale Weitzmann, PhD, Division of Endocrinology & Metabolism & Lipids, Emory University School of Medicine, 101 Woodruff Circle, 1305 WMB, Atlanta, Georgia 30322-0001, USA. E-mail: [mweitzm@emory.edu](mailto:mweitzm@emory.edu)

Roser-Page and Weiss contributed equally to the experimental execution of the work.

JBMR<sup>®</sup> Plus (WOA), Vol. 6, No. 7, July 2022, e10636.

DOI: 10.1002/jbm4.10636

© 2022 The Authors. *JBMR Plus* published by Wiley Periodicals LLC on behalf of American Society for Bone and Mineral Research.

induce their differentiation into FoxP3<sup>+</sup> immunosuppressive CD8<sup>+</sup> regulatory T cells (Tregs)<sup>(9)</sup> that function to limit bone resorption in ovariectomized mice<sup>(10)</sup> as well as stimulate bone formation.<sup>(9)</sup>

In contrast to anti-catabolic activities of CD8<sup>+</sup> T cells, our group has reported that the bone anabolic activity of parathyroid hormone (PTH) in mice, and of teriparatide in humans<sup>(11)</sup> is dependent in part, on production of the bone anabolic factor Wnt-10b by CD8<sup>+</sup> T cells.<sup>(12–14)</sup> PTH has further been reported to mediate regenerative effects in human periodontal ligament cells via Wnt-10b production.<sup>(15)</sup>

Abatacept is a pharmacological immunosuppressant, used in the therapy of chronic inflammatory states including rheumatoid arthritis and transplant rejection. Abatacept is based on the physiological CD28 co-stimulation inhibitor, cytotoxic T-lymphocyte antigen-4 (CTLA-4) a major product of activated T cells and Tregs. CTLA-4 mediates anti-resorptive activity, by virtue of its immunosuppressive action, in PTH-induced bone loss,<sup>(16)</sup> but has also been reported to directly bind to osteoclast precursors in vitro, inhibiting their differentiation.<sup>(17)</sup>

Interestingly, we have reported that abatacept is not only anti-resorptive, but in healthy wild-type (WT) mice stimulates bone formation and bone accrual, by driving Wnt-10b secretion by T cells.<sup>(18,19)</sup> This effect is counterbalanced by a negative feedback loop involving sclerostin production following blockade of CD80/86 ligands on osteoblast-lineage cells.<sup>(19)</sup>

We have uncovered a similar paradigm, in which the T cell CD40 ligand inhibitor MR1 induced gain of trabecular bone mass in the spine due to an increase in bone formation, that was associated with increased Treg development and elevated production of CTLA-4, leading to Wnt-10b production by T cells.<sup>(20)</sup>

At the molecular level, the mechanisms by which Wnt-10b is generated by CD28 co-stimulation blockade in T cells is unclear; however, the cAMP signal transduction pathway plays a key regulatory role in the process of T cell activation.<sup>(21,22)</sup> cAMP is generated following engagement of the T cell receptor (TCR) with antigen, presented by antigen presenting cells (APCs). cAMP signaling contributes to driving T cells to anergy, a dormant state, unless the cAMP signal is reversed through co-stimulation by CD28, a receptor on T cells that is activated by CD80/86 ligands expressed by APC. CD28 signaling activates a phosphodiesterase (PDE) in the T cell that catabolizes cAMP to inactive AMP, thus allowing T cell activation, proliferation, differentiation, and ultimately, downstream effector functions.<sup>(21,23–25)</sup>

cAMP is an activator of protein kinase A (PKA) that phosphorylates and activates the cAMP response element-binding protein (CREB), a transcription factor which associates with cAMP response elements (CREs) in the promoters of certain genes, including those involved in T cell activation such as IL-2.<sup>(26)</sup> Because cAMP has been reported to regulate basal Wnt-10b expression in adipocytes,<sup>(27)</sup> the premise of this study was that the cAMP/PKA/CREB pathway may also contribute to Wnt-10b production by CD8<sup>+</sup> T cells.

PDE inhibitors such as pentoxifylline (PTX) and rolipram, which block cAMP catabolism enhancing intracellular concentrations of cAMP, have long been recognized as stimulators of bone formation<sup>(28)</sup> and have recently come under renewed attention as potential bone regenerative agents.<sup>(29–32)</sup> However, the mechanisms by which PDE inhibitors induce bone formation have not been clarified, although it has been suggested that they may function by mimicking the downstream actions of PTH on osteoblasts, or by suppressing production of TNF $\alpha$  by macrophages,<sup>(28)</sup> a factor known to suppress bone formation.<sup>(33)</sup>

Indeed, recent studies in vitro using monocytes and peripheral blood mononuclear cells from human psoriatic arthritis patients, suggest that apremilast, a US Food and Drug Administration (FDA) approved PDE4 inhibitor, used for treatment of psoriatic arthritis, may inhibit osteoclastogenesis by suppressing production of inflammatory cytokines including TNF $\alpha$  and IL-17A.<sup>(34)</sup> Other in vitro studies have reported that PTX induces vascular endothelial growth factor, which could play a role in promoting bone formation directly.<sup>(29)</sup>

In the present study, we investigated the mechanisms underlying the bone anabolic response of the PDE inhibitor PTX in mice in vivo. Our data reveal that PTX induces a state of increased bone turnover with a net increase in bone mass in the axial skeleton, and that CD8<sup>+</sup> T cells and Wnt-10b are mandatory for this bone anabolic response. By contrast, PTX-induced bone resorption was independent of T cells, and was the dominant effect on bone in T cell-deficient mice.

## Materials and Methods

Pentoxifylline and all other reagents were purchased from the Millipore-Sigma Aldrich Chemical Co. (St. Louis, MO, USA), unless indicated.

### Mice

Animal studies were approved by both the Atlanta VA Medical Center and Emory University Animal Care and Use Committees and were conducted in accordance with the NIH Laboratory Guide for the Care and Use of Laboratory Animals.

Mice were housed under specific pathogen free conditions and fed 5V02 mouse chow (Purina Mills, St. Louis, MO, USA) and water ad libitum. The animal facility was kept at 23  $\pm$  1°C, with 50% relative humidity and a 12/12-hour light/dark cycle.

Female C57BL6/J WT mice and T cell receptor  $\beta$  gene (*Tcrb*) KO (TCR $\beta$  KO) mice lacking  $\alpha\beta$  T cells (B6.129P2-Tcrbtm1Mom/J) were purchased from the Jackson Laboratory (Bar Harbor, ME, USA). *Wnt-10b* gene KO mice (Wnt-10b KO) on the C57BL6 background were obtained from a breeding colony maintained at Emory University and were originally gifted by Dr. T.F. Lane (UCLA).<sup>(12,19,35)</sup> We used young mice (8 weeks of age) to maintain consistency with our previous studies of T cell-induced bone anabolism and because both young and skeletally mature mice respond to anabolic stimuli, but younger mice have greater statistical power to detect changes due to increased magnitude of responses.<sup>(18)</sup> We used  $n = 10–11$  mice/group based on our previous publications of CD8<sup>+</sup> T cell anabolism where  $n = 7–8$  mice/group<sup>(18,20)</sup> generated significant outcomes. Analyses were performed blinded to the nature of the samples. Animals were distributed into groups based on baseline total body bone mineral density (BMD) quantified by dual-energy X-ray absorptiometry (DXA) (PixiMus; GE Medical Systems, Milwaukee, WI, USA) to minimize variance between groups that could bias outcomes in cross-sectional endpoints. Group baseline total body BMD values (mean  $\pm$  SD, g/cm<sup>2</sup>) are as follows: Figs. 1 and 2: WT + vehicle (0.0426  $\pm$  0.0023); WT + PTX (0.0425  $\pm$  0.0018). Figures 3 and 4: TCR $\beta$  KO + vehicle (0.0459  $\pm$  0.0015); TCR $\beta$  + PTX (0.0458  $\pm$  0.0009); TCR $\beta$  KO + WT CD8<sup>+</sup> T cells + PTX (0.0457  $\pm$  0.0011) and TCR $\beta$  KO + Wnt-10b CD8<sup>+</sup> T cells + PTX (0.0465  $\pm$  0.0017). Percentage change between all groups within an experiment was less than 2%.

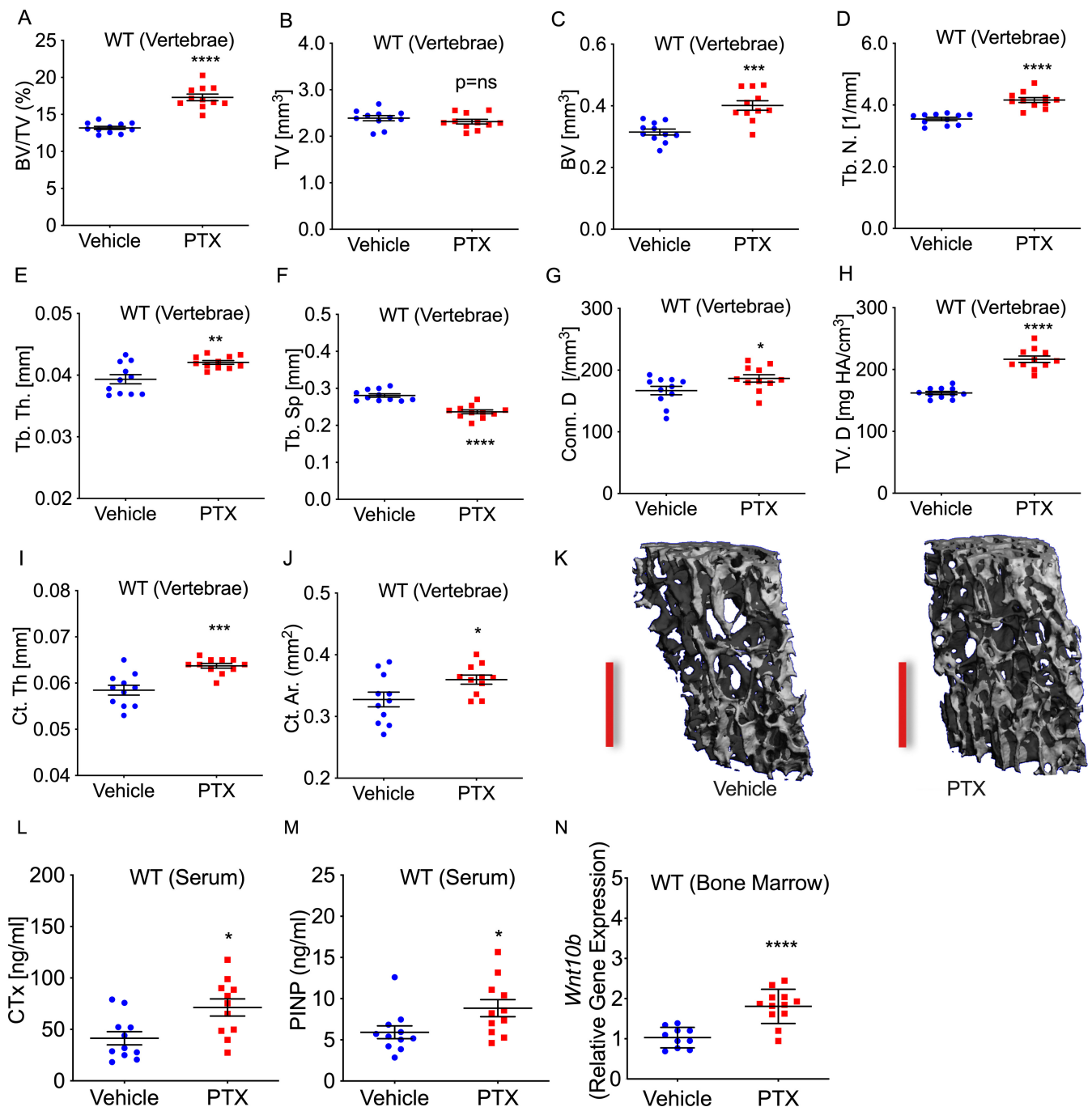


**Fig. 1.** PTX induces both bone formation and resorption in WT mice leading to increased lumbar spine trabecular and cortical bone mass. Two-month-old WT C57BL6/J female mice were treated with PTX or vehicle (PBS) 5 times/week, for 12 weeks. Vertebral ( $L_3$ ) trabecular and cortical structure was analyzed by  $\mu$ CT and serum bone turnover markers by ELISA.  $\mu$ CT trabecular indices: (A) BV/TV; (B) TV; (C) BV; (D) Tb.N; (E) Tb.Th; (F) Tb.Sp; (G) Conn.D; and (H) TV.D.  $\mu$ CT cortical indices: (I) Ct.Th and (J) Ct.Ar. (K) Representative 6- $\mu$ m  $\mu$ CT reconstructions of vertebrae for vehicle-treated and PTX-treated mice. Red scale bar = 500  $\mu$ m. (L) Bone resorption marker CTx and (M) bone formation marker P1NP. (N) RT-PCR analysis of *Wnt-10b* gene expression in bone marrow. Mean  $\pm$  SEM. \* $p < 0.05$ ; \*\* $p < 0.01$ , \*\*\* $p < 0.001$ , \*\*\*\* $p < 0.0001$ , or  $p = ns$  (not significant) by Student's *t* test or Mann-Whitney test (P1NP) following assessment for normal distribution by Shapiro-Wilk normality test.  $n = 11$  mice/group. One vehicle RT-PCR sample was undetectable in N. BV = bone volume; BV/TV = trabecular bone volume fraction; Conn.D = connectivity density; Ct.Ar = cortical area; Ct.Th = cortical thickness; CTx = C-terminal telopeptide of collagen type I; P1NP = N-terminal propeptide of type-I procollagen; Tb.N = trabecular number; Tb.Sp = trabecular separation; Tb.Th = trabecular thickness; TV = tissue volume; TV.D = volumetric bone density.

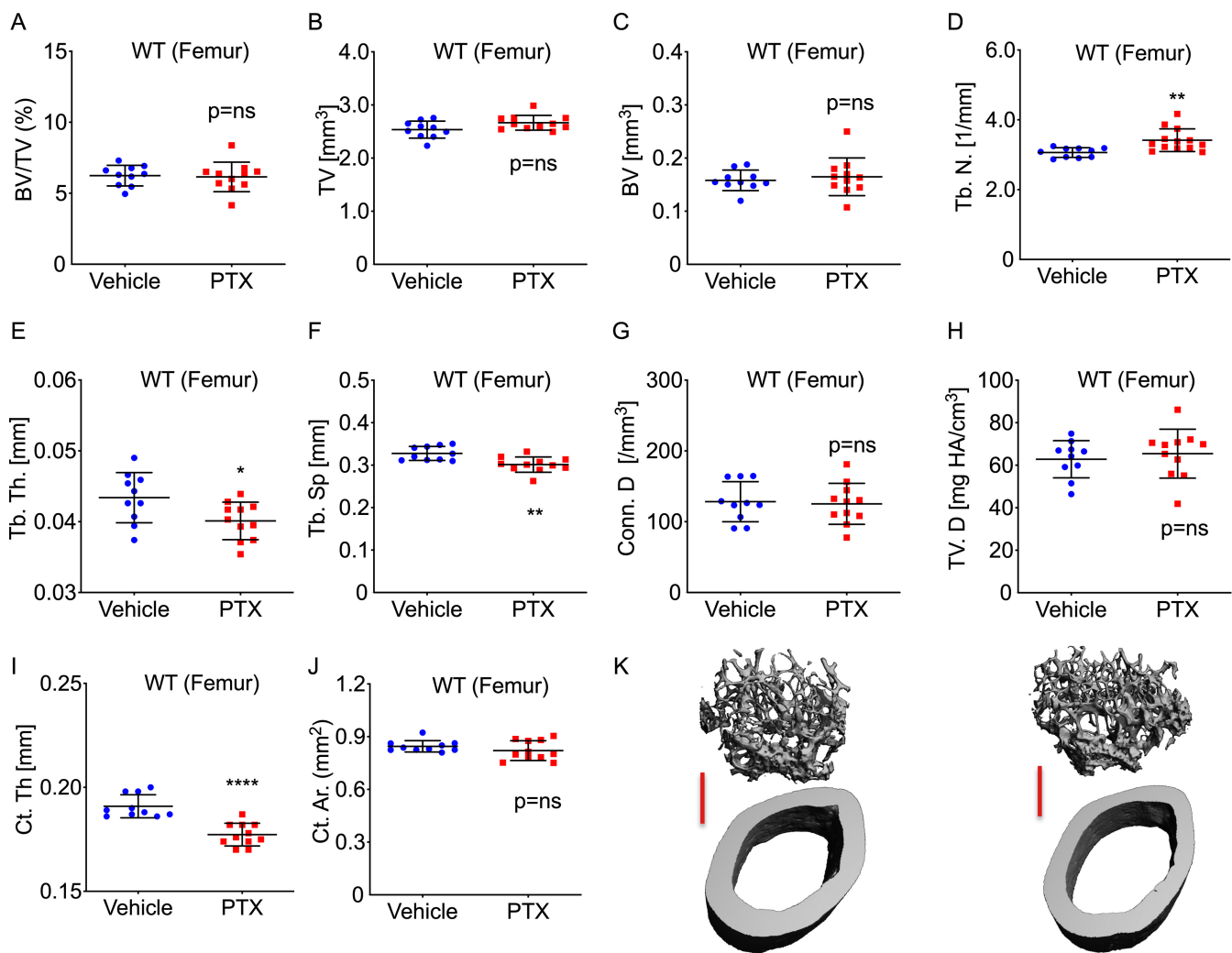


**Fig. 2.** PTX does not increase femoral trabecular and cortical bone mass in WT mice. Two-month-old healthy intact WT C57BL6/J female mice were treated with PTX or vehicle (PBS) 5 times/week, for 12 weeks and femoral bone analyzed by  $\mu$ CT. Trabecular bone indices: (A) BV/TV; (B) TV; (C) BV; (D) Tb.N; (E) Tb. Th; (F) Tb.Sp; (G) Conn.D; and (H) TV.D. Cortical indices: (I) Ct.Th and (J) Ct.Ar. (K) Representative 6- $\mu$ m  $\mu$ CT reconstructions of the femur are shown for vehicle-treated and PTX-treated mice with trabecular bone on top and cortical bone below. Red scale bar = 500  $\mu$ m. Mean  $\pm$  SEM. \* $p < 0.05$ ; \*\* $p < 0.01$ , \*\*\* $p < 0.001$ , or  $p = ns$  (not significant) by Student's  $t$  test or Mann-Whitney test (Tb.N, Ct.Th, and Ct.Ar) following assessment for normal distribution by Shapiro-Wilk normality test.  $n = 11$  mice/group. One femur in the vehicle group was damaged and could not be analyzed. BV = bone volume; BV/TV = trabecular bone volume fraction; Conn.D = connectivity density; Ct.Ar = cortical area; Ct.Th = cortical thickness; CTx = C-terminal telopeptide of collagen type I; P1NP = N-terminal propeptide of type-I procollagen; Tb.N = trabecular number; Tb.Sp = trabecular separation; Tb.Th = trabecular thickness; TV = tissue volume; TV.D = volumetric bone density.

### PTX administration to mice

Mice were injected daily (Monday to Friday) for 12 weeks with PTX (50 mg/kg/d) by intraperitoneal injection (i.p.). Control mice were injected with vehicle (phosphate-buffered saline [PBS]). We elected to use a pharmacological dose used in humans to treat claudication (400 mg/d), which we allometrically scaled (3/4 power scaling) for mouse metabolic equivalency<sup>(36)</sup> to  $\sim 50$  mg/kg/d.

### T cell adoptive transfer

To test the specific role of Wnt-10b from CD8<sup>+</sup> T cells in the response to PTX we generated chimeric mice unable to express

Wnt-10b from their CD8<sup>+</sup> T cells, but with all other sources of Wnt-10b intact, as described.<sup>(12,37–39)</sup> Briefly, WT or Wnt-10b KO CD8<sup>+</sup> T cells were isolated from the spleens of 6-week-old to 8-week-old female mice using EasySep negative immunomagnetic purification (StemCell Technologies Inc., Kent, WA, USA). Purified CD8<sup>+</sup> T cells ( $2 \times 10^6$ /mouse) were adoptively transferred by tail vein injection into female C57BL6/J TCR $\beta$  KO mice at 8 weeks of age. Sham mice were tail vein injected with vehicle (PBS).

### Real-time RT-PCR

Whole bone marrow was purified from a single tibia and the pelvis and *Wnt-10b* expression analysis was performed as

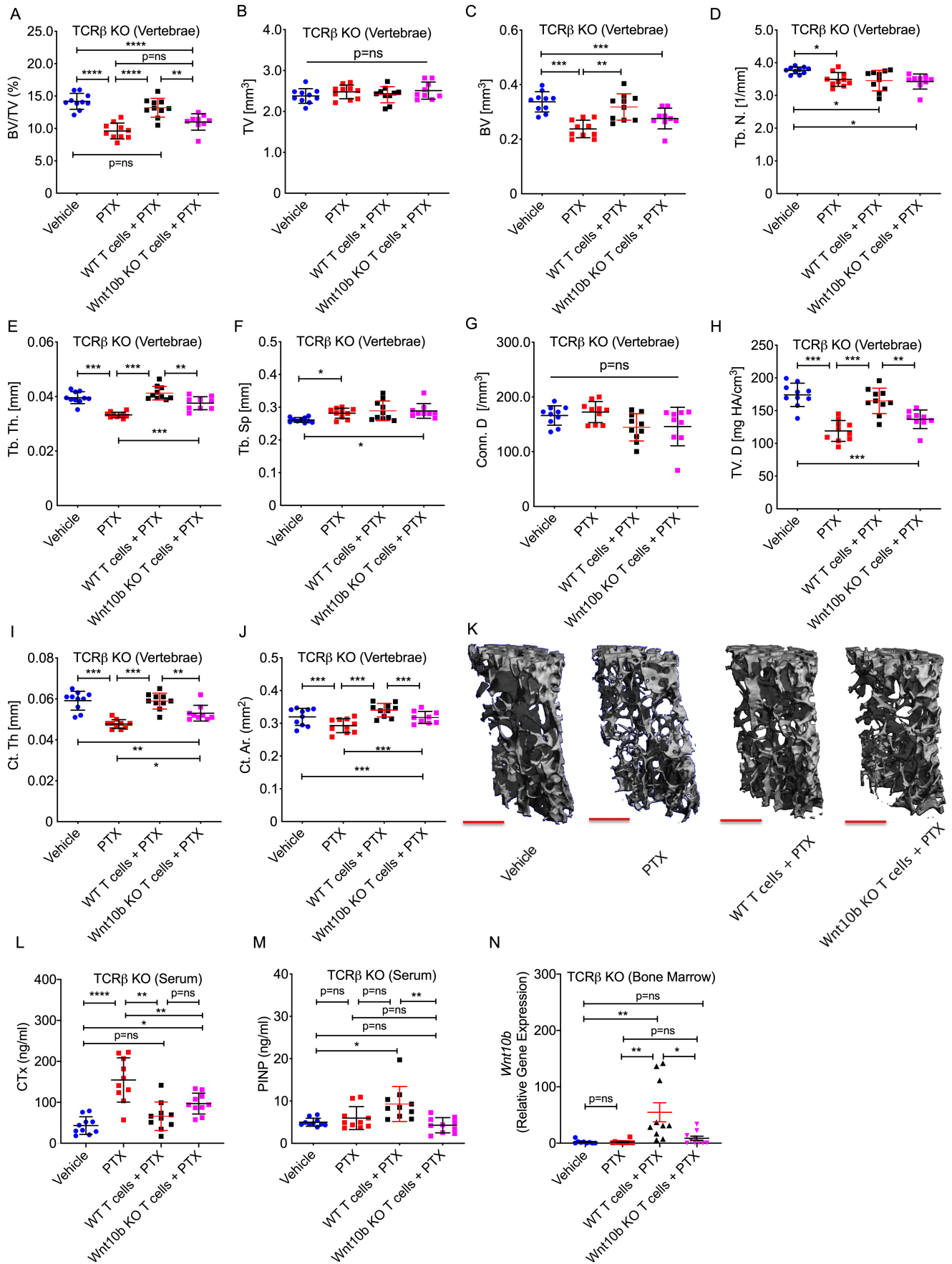




**Fig. 3.** PTX induces vertebral bone loss due to increased resorption, but not formation, in T cell–deficient mice, but is rescued by reconstitution of CD8<sup>+</sup> T cells from WT, but not Wnt-10b KO mice. C57BL6/J female TCRβ KO T cell–deficient mice, and TCRβ KO mice reconstituted with WT or CD8<sup>+</sup> Wnt-10b KO T cells, were treated with PTX or vehicle (PBS) 5 times/week, for 12 weeks. Vertebral structural indices were analyzed by μCT for: (A) BV/TV; (B) TV; (C) BV; (D) Tb.N; (E) Tb.Th; (F) Tb.Sp; (G) Conn.D; and (H) TV.D, and for cortical indices: (I) Ct.Th and (J) Ct.Ar. (K) Representative 6-μm μCT reconstructions. Red scale bar = 500 μm. (L) Bone resorption marker C-terminal telopeptide of CTx and (M) bone formation marker P1NP. (N) RT-PCR analysis of *Wnt-10b* expression in bone marrow. Mean ± SEM. \**p* < 0.05; \*\**p* < 0.01, \*\*\**p* < 0.001, \*\*\*\**p* < 0.001, or *p* = ns (not significant) by one-way ANOVA or Kruskal-Wallis test (BV/TV, Tb.N, Tb.Sp, Conn. D, TV.D, and Ct.Th). *n* = 10 mice/group. One extreme outlier in the Wnt-10b KO T cells + PTX group, with an exceptionally high BV/TV (=17%) and other parameters was excluded from the μCT data. BV = bone volume; BV/TV = trabecular bone volume fraction; Conn.D = connectivity density; Ct. Ar = cortical area; Ct.Th = cortical thickness; CTx = C-terminal telopeptide of collagen type I; P1NP = N-terminal propeptide of type-I procollagen; Tb. N = trabecular number; Tb.Sp = trabecular separation; Tb.Th = trabecular thickness; TV = tissue volume; TV.D = volumetric bone density.

described<sup>(18)</sup> on an ABI Prism 7000 instrument (Applied Biosystems, Foster City, CA, USA) using Applied Biosystems master mix and primer sets and probes for murine *Wnt-10b* (Mm00442104). Fold changes were calculated using the 2<sup>−ΔΔCt</sup> method<sup>(22)</sup> with normalization to *β-actin* (Mm 00607939). To quantify the effect of cAMP pathway activators and inhibitors on Wnt-10b, RT-PCR was performed as described<sup>(40)</sup> using SYBR green Master Mix (Applied Biosystems) and *Wnt-10b* mRNA normalized to 18S rRNA, using previously validated primers.<sup>(40)</sup>

#### Wnt-10b-promoter reporter assays

Wnt-10b-promoter luciferase assays were performed as described.<sup>(40)</sup> A plasmid containing a −705 to +216 bp DNA sequence of the mouse Wnt-10b-promoter was kindly provided by Dr. D. J. Klemm (University of Colorado).<sup>(27)</sup> CD8<sup>+</sup> T cells were

purified from disaggregated spleen by negative selection Easy-Sep Mouse CD8<sup>+</sup> T cell Isolation Kit (StemCell Technologies Inc.) and transfected using an Amaxa Mouse T Cell Nucleofactor Kit (Lonza, Basel, Switzerland) with 3.6 μg of empty vector (pGL3-basic) or Wnt-10b-reporter construct and 0.4 μg TK-pRL Renilla transfection control vector. Twenty-four hours after transfection cells were stimulated with plate-bound anti-CD3e (10 μg/mL) and soluble anti-CD28 activating antibodies (25 μg/mL) from BioLegend (San Diego, CA, USA). PTX (100 μM) and other activators and inhibitors of the cAMP/PKA/CREB pathway included: H89 a PKA inhibitor (25 μM in dimethylsulfoxide [DMSO]); 666-15 (1 μM in DMSO) a CREB inhibitor, and the PDE inhibitor PTX (100 μM in PBS), and apremilast (10 μM in DMSO) a PDE4 inhibitor, all from R&D Systems, Minneapolis, MN, USA). After 6 hours, luciferase activity was quantified using a dual-luciferase reporter assay kit (Promega BioSciences, San

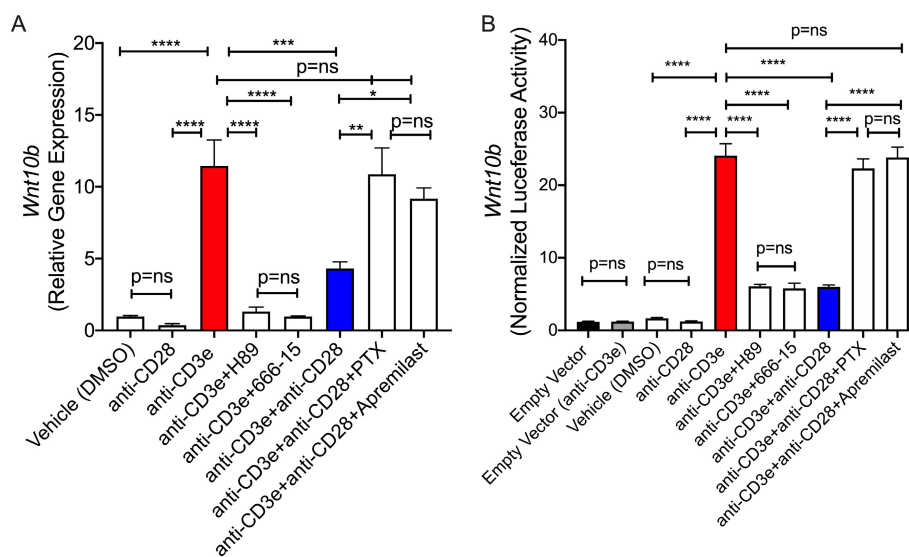


**Fig. 4.** In vitro analysis of the role of the cAMP pathway in *Wnt-10b* expression by CD8<sup>+</sup> T cells. The effect of cAMP pathway activators and inhibitors on *Wnt-10b* gene expression in purified CD8<sup>+</sup> T cells was assessed by (A) RT-PCR and (B) by luciferase assay using a transfected Wnt-10b promoter reporter and normalized to Renilla. In both (A) and (B) purified T cells were stimulated with plate bound anti-CD3e (10 μg/mL) and/or soluble anti-CD28 activating antibodies (25 μg/mL). Cells were treated with the inducers of cAMP accumulation (PTX [100 μM] and apremilast [10 μM]) or with H89 (25 μM) an inhibitor of PKA or 666-15 (1 μM) a CREB inhibitor. After 6 hours (A) mRNA was extracted for RT-PCR quantification of *Wnt-10b* expression with normalization to 18S, or (B) quantification of luciferase activity using a dual-luciferase reporter assay with normalization for Renilla expression. Mean ± SEM. \**p* < 0.05; \*\**p* < 0.01, \*\*\**p* < 0.001, \*\*\*\**p* < 0.001, or *p* = ns (not significant) by one-way ANOVA following assessment for normal distribution by Shapiro-Wilk normality test. *n* = 4 replicates/group and the data are representative of two independent experiments.

Luis Obispo, CA, USA) on a Turner BioSystems Inc. (Sunnyvale, CA, USA) luminometer and data normalized for Renilla expression.

### Micro-computed tomography

Micro-computed tomography ( $\mu$ CT) was performed in L<sub>3</sub> vertebrae and the distal femoral metaphysis using a  $\mu$ CT40 scanner (Scanco Medical AG, Brüttisellen, Switzerland) as described.<sup>(18,20)</sup> We scanned 405 tomographic slices at a voxel size of 6  $\mu$ m (70 kVp and 114 mA, and with 200 ms integration time) at the L<sub>3</sub> vertebra (total length of 2.4 mm) and 100 tomographic slices at the distal femoral metaphysis. Trabecular bone was segmented from the cortical shell for a total length of 0.6 mm beginning 0.5 mm from the distal growth plate. Cortical bone was quantified at the femoral mid-diaphysis from 100 tomographic slices (total length of 0.6 mm). We used the thresholding approach described by Buxsein and colleagues,<sup>(41)</sup> which is recommended by the  $\mu$ CT manufacturer, and involves a visual inspection and comparison of preview and slice wise grayscale two-dimensional (2D) images. The same threshold value was used for all measurements.

### Quantitative bone Histomorphometry

Bone histomorphometry was performed by the Center for Metabolic Bone Disease-Histomorphometry and Molecular Analysis Core Laboratory of the University of Alabama at Birmingham, on trichrome-stained plastic-embedded sections of calcein labeled femurs from vehicle and PTX-injected mice. For dynamic bone formation indices mice were injected subcutaneously with calcein at day 10 and day 3 before euthanasia.

### Biochemical indices of bone turnover

Serum biochemical markers of bone resorption (C-terminal telopeptide of collagen [CTx]) and of bone formation (N-terminal propeptide of type I procollagen [P1NP]) were quantified in mice serum using ELISAs from Immunodiagnostic Systems Inc. (Gaithersburg, MD, USA).

### Statistical analysis

Statistical significance was determined using Prism version 8.4.3 for Macintosh (GraphPad Software Inc., La Jolla, CA, USA). Gaussian distribution was assessed by Shapiro-Wilk test. Parametric two sample comparisons were made using unpaired two-tailed Student's *t* test. Welch's correction was applied to samples with unequal variance based on *F*-test. For nonparametric data Mann-Whitney test was used. Multigroup comparisons ( $\geq 3$ ) were made using one-way ANOVA with Tukey-Kramer post hoc test for parametric data, or Kruskal-Wallis test with Dunn's post hoc test, for nonparametric data. Outliers were assessed by Grubb's test with  $\alpha = 0.05$ . All available data were used for analysis unless otherwise stated in the figure legend. Graphical data are presented as mean  $\pm$  standard error of the mean (SEM) with dots representing individual mice;  $p < 0.05$  was considered statistically significant.

## Results

### Treatment of WT mice with PTX increases trabecular and cortical parameters of bone mass in the lumbar spine

To investigate the net effect of cAMP elevation *in vivo*, we treated healthy WT female C57BL6/J mice, 8 weeks of age, with PTX, a potent broad-spectrum PDE inhibitor, or with vehicle (PBS). Mice were injected i.p. five times/week, for 12 weeks and L<sub>3</sub> lumbar vertebrae were analyzed by  $\mu$ CT to obtain separate high-resolution microarchitectural analyses of the trabecular and cortical compartments.

Trabecular bone volume fraction (BV/TV) a key index of trabecular bone mass, was significantly increased in PTX-treated WT mice (Fig. 1A). This was a consequence of increased bone volume (BV) rather than a change in tissue volume (TV), an index reflecting changes in trabecular compartment size (Fig. 1B,C). The structural indices trabecular number (Tb.N) and trabecular thickness (Tb.Th) were both significantly increased by PTX treatment (Fig. 1D,E), consistent with a corresponding decline in trabecular separation (Tb.Sp) (Fig. 1F). Connectivity density (Conn.D) and volumetric bone density (TV.D) measurements were also significantly increased (Fig. 1G,H).

Two key indices of cortical mass: cortical area (Ct.Ar) and cortical thickness (Ct.Th), were significantly increased by PTX treatment (Fig. 1I,J). Representative  $\mu$ CT reconstructions of L<sub>3</sub> vertebrae are shown for vehicle-treated and PTX-treated WT mice (Fig. 1K).

### Biochemical indices of bone formation and resorption are increased in PTX-treated WT mice

To assess PTX-induced bone turnover we examined changes in bone resorption and bone formation by quantifying serum biochemical markers of bone resorption (CTx) and of bone formation (P1NP). Both CTx (Fig. 1L) and P1NP (Fig. 1M) were significantly increased in PTX-treated WT mice. The data suggest a high rate of bone turnover (increased formation and resorption) but with net gain in BV/TV in the axial skeleton (Fig. 1A).

### Wnt-10b expression in the bone marrow is increased in PTX-treated WT mice

We have previously reported that T cells activated in the absence of CD28 co-stimulation *in vitro* express *Wnt-10b*, which could account for the bone anabolic activity of abatacept in mice.<sup>(18,19)</sup> To investigate whether PTX promotes *Wnt-10b* expression, we performed RT-PCR in whole bone marrow from vehicle-treated and PTX-treated WT mice. The data reveal a significant increase in *Wnt-10b* expression in PTX-treated mice (Fig. 1N).

### Treatment of healthy WT mice with PTX fails to increase trabecular and cortical parameters of bone mass in the femur

In contrast to the vertebrae, BV/TV in the femur was not significantly increased by PTX (Fig. 2A), although interestingly, Tb.N was significantly increased whereas Tb.Th was significantly diminished (Fig. 2D,E). Tb.Sp was modestly decreased (Fig. 2F), whereas TV and BV (Fig. 2B,C) and Conn.D and TV.D (Fig. 2G,H) were unchanged. In the cortical compartment, Ct.Th was significantly diminished but Ct.Ar remained unchanged (Fig. 2I,J).

Representative  $\mu$ CT reconstructions of femoral cortical and trabecular bone are shown for vehicle-treated and PTX-treated WT mice (Fig. 2K).

#### Analysis of PTX-treated WT femurs by histomorphometry

Histomorphometry performed on isolated calcein labeled femurs from vehicle-treated and PTX-treated WT mice revealed no significant changes in osteoclast surface normalized for bone surface (Oc.S/BS); however, the number of osteoclasts (N.Oc/BS) were significantly increased (Table 1).

Neither the static indices osteoblast surface (Ob.S/BS) and the number of osteoblasts (N.Ob/BS), nor the dynamic indices mineral apposition rate (MAR) and bone formation rate (BFR/BS) were significantly changed by PTX treatment in the femur (Table 1), consistent with a lack of BV/TV increase at this site.

#### PTX induces bone loss in T cell-deficient TCR $\beta$ KO mice, but bone loss is rescued by reconstitution of TCR $\beta$ KO mice with CD8 $^{+}$ T cells from WT, but not by reconstitution of TCR $\beta$ KO mice with CD8 $^{+}$ T cells from Wnt-10b KO mice

To further explore the role of CD8 $^{+}$  T cells, and their Wnt-10b production, in the bone anabolic and catabolic effects of PTX, we administered PTX to TCR $\beta$  KO mice lacking  $\alpha\beta$  T cells, the TCR expressed by the vast majority of T cells in the body. To demonstrate the specific role of Wnt-10b production from CD8 $^{+}$  T cells in the bone anabolic effect of PTX we also reconstituted, by adoptive transfer, TCR $\beta$  KO mice with CD8 $^{+}$  T cells derived from Wnt-10b KO mice. Control mice were reconstituted with WT CD8 $^{+}$  T cells.

Using  $\mu$ CT to assess changes in vertebral bone mass, we found that PTX not only failed to promote trabecular bone accretion in the TCR $\beta$  KO mice, but BV/TV, BV, Tb.N, Tb.Th, and TV.D were all significantly diminished by PTX treatment (Fig. 3A,C-E). Consistent with the decline in BV/TV, Tb.Sp was increased (Fig. 3F), while TV and Conn.D were not significantly affected by PTX treatment (Fig. 3B,G).

Adoptive transfer of WT CD8 $^{+}$  T cells into TCR $\beta$  KO mice rescued mice from trabecular bone loss; however, TCR $\beta$  KO mice transplanted with T cells lacking expression of Wnt-10b, were not protected from bone loss (Fig. 3A,C,D,H).

Similar to the trabecular compartment, the key cortical indices Ct.Th and Ct.Ar were significantly decreased by PTX treatment in mice lacking CD8 $^{+}$  T cells (Fig. 3I,J) and WT CD8 $^{+}$  T cells reversed these changes. By contrast, transplantation of Wnt-10b KO CD8 $^{+}$  T cells into TCR $\beta$  KO mice only partly reversed the changes in Ct.

Th and Ct.Ar (Fig. 3J). Representative  $\mu$ CT reconstructions of L<sub>3</sub> vertebrae are shown for each group (Fig. 3K).

#### Biochemical indices of bone resorption, but not bone formation, are increased by PTX treatment of T cell-deficient TCR $\beta$ KO mice

The biochemical marker of bone resorption CTx, reflected enhanced bone resorption induced by PTX in T cell-deficient mice and was significantly reversed by transplantation of WT CD8 $^{+}$  T cells and partly reversed by Wnt-10b KO CD8 $^{+}$  T cells (Fig. 3L). Bone formation marker P1NP was not increased by PTX treatment of TCR $\beta$  KO mice, but was rescued by transplantation of WT, but not Wnt-10b KO CD8 $^{+}$  T cells (Fig. 3M).

#### Wnt-10b expression in the bone marrow is not increased by PTX treatment of TCR $\beta$ KO mice, but is rescued by reconstitution of WT, but not Wnt-10b KO, CD8 $^{+}$ T cells

Consistent with the hypothesis that CD8 $^{+}$  T cells are the relevant source of PTX-induced Wnt-10b, Wnt-10b expression in the bone marrow was not increased in PTX-treated TCR $\beta$  KO mice, but was rescued by transplantation of TCR $\beta$  KO mice with WT, but not Wnt-10b KO CD8 $^{+}$  T cells (Fig. 3N).

Taken together, these data suggest that the bone anabolic effects (increased P1NP and vertebral BV/TV increase) induced by PTX are mediated through CD8 $^{+}$  T cells and specifically through Wnt-10b production by CD8 $^{+}$  T cells. By contrast, T cells are dispensable for the bone catabolic action (increased CTx in WT and TCR $\beta$  KO mice, and BV/TV loss in TCR $\beta$  KO mice) induced by PTX, and counteract in part, the magnitude of the resorptive activity of PTX.

#### Wnt-10b gene expression is upregulated in WT CD8 $^{+}$ T cells activated in the absence of CD28 co-stimulation and in dual CD3-activated and CD28-activated CD8 $^{+}$ T cells treated with PDE inhibitors, whereas inhibitors of PKA and CREB suppress Wnt-10b expression

To investigate the molecular signals that drive Wnt-10b expression in CD8 $^{+}$  T cells, we treated purified primary WT CD8 $^{+}$  T cells with inhibitors and activators of the cAMP pathway and quantified Wnt-10b gene expression by RT-PCR. Activation of T cells by CD3 activation (using an anti-CD3e activating antibody) in the absence of CD28 co-stimulation led to significant induction of Wnt-10b gene expression (Fig. 4A; red bar). As expected, Wnt-10b expression was significantly diminished by CD28 co-stimulation in CD3-activated T cells (Fig. 4A; blue bar).

**Table 1.** Histomorphometry of Vehicle-Treated and PTX-Treated Mice (Femur)

Parameters	Vehicle-treated (mean $\pm$ SD)	PTX-treated (mean $\pm$ SD)	Percent change	<i>p</i>
<b>Static indices</b>				
Oc.S/BS	5.243 $\pm$ 2.115	6.332 $\pm$ 2.297	20.8	0.1043
N.Oc/BS	1.815 $\pm$ 0.623	2.243 $\pm$ 0.706	23.6	0.0315
Ob.S/BS	40.478 $\pm$ 9.955	42.485 $\pm$ 10.137	5.0	0.4603
N.Ob/BS	30.157 $\pm$ 5.807	30.885 $\pm$ 6.737	2.4	0.6719
<b>Dynamic indices</b>				
MAR ( $\mu$ m/d)	1.272 $\pm$ 0.192	1.304 $\pm$ 0.276	2.5	0.6608
BFR/BS ( $\mu$ m/d)	0.524 $\pm$ 0.082	0.458 $\pm$ 0.118	-12.6	0.0607

Values of *p* represent Student's *t* tests. *n* = 11 mice/group. Percent change is the percentage change between the vehicle-treated and PTX-treated group.

BFR = bone formation rate; BS = bone surface; MAR = mineral apposition rate; N.Ob = osteoblast number; N.Oc = osteoclast number; Ob.S = osteoblast surface; Oc.S = osteoclast surface.



Suppression of cAMP degradation using the broad-spectrum PDE inhibitor PTX, or the PDE4-specific inhibitor apremilast, both reversed the suppressive effect of dual CD3 and CD28-induced T cell activation, on *Wnt-10b* gene expression. CD3-induced *Wnt-10b* expression was significantly suppressed by the PKA inhibitor H89 and by the CREB activation inhibitor 666-15 (Fig. 4A), attesting to a role for these downstream cAMP-signal transduction mediators.

Finally, we interrogated *Wnt-10b* gene activation in WT CD8<sup>+</sup> T cells using a *Wnt-10b* promoter-luciferase reporter construct that was transfected into purified primary CD8<sup>+</sup> T cells and treated with activators and inhibitors of the cAMP pathway, as described above for the RT-PCR study, following activation in the presence or absence of CD28 co-stimulation. This study produced almost identical outcomes to those reported above for mRNA quantification (Fig. 4B) and support a direct role of the cAMP pathway in *Wnt-10b* promoter activation.

## Discussion

The cAMP signal transduction pathway is recognized as a key suppressor of T cell activation,<sup>(22)</sup> and promotes a state recognized to stimulate *Wnt-10b* secretion and bone anabolism.<sup>(18)</sup> In this study, we examined the cellular and molecular mechanisms by which the pharmacological PDE inhibitor PTX drives bone anabolic activity. Our data confirm the bone anabolic potential of PDE inhibition and demonstrate a previously unrecognized requirement for CD8<sup>+</sup> T cells, and for *Wnt-10b* production, in PTX-induced bone formation. A key role for CD8<sup>+</sup> T cells was evidenced by the loss of bone anabolic activity in T cell KO mice and restoration of bone formation by transplantation of WT CD8<sup>+</sup> T cells. By contrast, reconstitution by CD8<sup>+</sup> T cells lacking a functional *Wnt-10b* gene, failed to restore bone formation, corroborating a specific role for this bone anabolic *Wnt* ligand in PTX-induced bone anabolism. In vitro molecular signaling studies further demonstrate that activation of the cAMP signal transduction pathway in CD8<sup>+</sup> T cells drives *Wnt-10b* transcription through classical downstream cAMP mediators including PKA and CREB.

Administration of PTX to WT mice resulted in a high bone turnover state characterized by accelerated bone formation and bone resorption, which competed against each other. Over an extended period of 3 months, the balance of bone resorption and formation was in favor of trabecular and cortical bone volume gain in the axial skeleton. By contrast, we did not observe significant bone acquisition in the femur and although PTX appeared to promote an increase in femoral Tb.N, this was offset by a simultaneous decline in Tb.Th. The opposing actions of formation and resorption may have led to an expansion of new trabecular bone elements through increased bone formation, but with denuding of existing element thickness through competing bone resorption. An alternative explanation for increased Tb.N, in the face of diminished Tb.Th, is that elevated bone resorption can lead to the perforation of trabecular rods, leading to an apparent increase in rod number. This latter explanation is consistent with our histomorphometry which revealed a significant increase in the N.Oc/BS while the N.Ob/BS was not significantly increased, suggesting that the dominant activity in the femur at the time of mice euthanasia was pro-resorptive, rather than anabolic.

In the absence of T cells (TCR $\beta$  KO mice), the net effect of PTX was bone loss, the result of induced bone resorption in the face

of a stagnant anabolic response. As loss of T cells failed to abrogate the pro-resorptive effects of PTX, the data suggest that T cells are obligatory for PTX-induced bone anabolism, but are dispensable for PTX-induced bone resorption. This is consistent with previous studies reporting that PDE inhibitors such as PTX, may upregulate RANKL production by osteoblasts.<sup>(42)</sup>

Unlike previous studies using PTX in intact WT animals<sup>(28)</sup> that were found to be bone anabolic in the femur, the balance of formation and resorption in our study led to significant bone gain in the vertebrae only. The reason for this is unclear, but interestingly, we previously observed a similar predilection for bone gain in the vertebrae when we treated mice with an antibody that inhibits CD40 ligand co-stimulation.<sup>(20)</sup> Furthermore, clinical studies have revealed that the axial skeleton undergoes a much more robust response to teriparatide than the appendicular skeleton.<sup>(43)</sup>

One explanation for this is that the size of the CD8<sup>+</sup> T cell pool in C57BL6 mice is almost 60% greater in the vertebrae than in femoral bone marrow.<sup>(44)</sup> This expanded number of CD8<sup>+</sup> T cells in the vertebrae may have been sufficient to sustain an anabolic response, while the lower total number of CD8<sup>+</sup> T cells in the femur may have been inadequate to meet the threshold concentration of *Wnt-10b* required to promote sufficient bone formation to overcome the direct effects of PTX on osteoclastic bone resorption.

Another difference is that the previous study used a higher dose of PTX (100–200 mg/kg),<sup>(28)</sup> while our study used 50 mg/kg/d, a dose allometrically scaled to mouse equivalency from the clinical dose used to ameliorate claudication in humans. We chose this lower dose because, in a pilot study performed in preparation for our experiments, we found that PTX doses >50 mg/kg caused the mice to display symptoms of illness, such as lethargy. Indeed, systemic global PDE inhibitors, such as PTX and rolipram, are used sparingly in humans because they are associated with similar side effects. Although we did not observe obvious signs of lethargy in our study, it is possible that animal activity may have been diminished, causing reduced biomechanical loading of the femurs, relative to control mice that may have favored resorption over formation at this site.

Although *Wnt-10b* expression in bone marrow was significantly elevated in response to PTX (Fig. 1N), there was no significant difference in BV/TV and bone formation by histomorphometry, in the femur. A likely explanation for this is that bone marrow for RT-PCR studies was derived predominantly from the marrow-rich pelvis and this bone marrow may more closely represent vertebral bone marrow than femoral bone marrow, in terms of the numbers and/or distribution/localization of CD8<sup>+</sup> T cells.

Another apparent discrepancy is that the bone turnover markers suggest that both formation and resorption were promoted by PTX, whereas the histomorphometry only revealed increases in the N.Oc/BS. The likely explanation is that as evidenced by the  $\mu$ CT data, bone formation in the femur was muted and did not lead to a significant increase in bone volume. Another possible explanation for osteoblast numbers not being increased is that preexisting osteoblasts may have been transiently activated, rather than de novo formation of new osteoblasts. This may have been sufficient to offset a slight increase in bone resorption, but inadequate to promote an increase in volume.

Although reconstitution of WT CD8<sup>+</sup> T cells rescued PTX-induced bone loss and restored bone formation, BV/TV was not significantly increased in the vertebrae relative to untreated

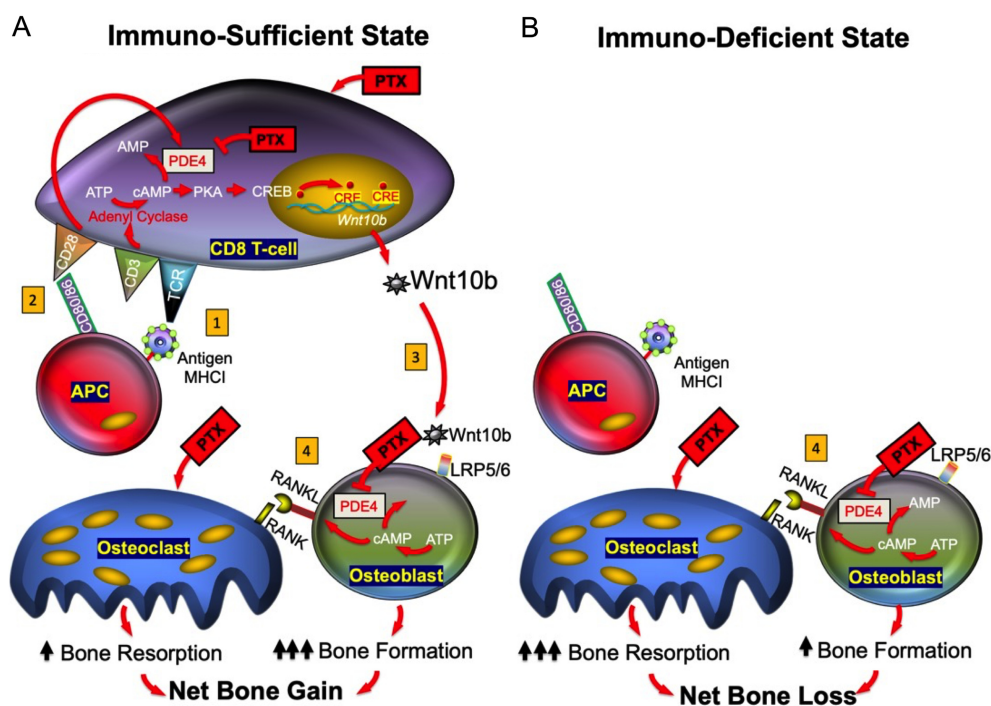


**Fig. 5.** Model for PDE-induced bone anabolism by CD8<sup>+</sup> T cells. (A) Under immunosufficient conditions, (1) APCs present antigen to the TCR activating the associated CD3 complex (signal 1) and leading to activation of adenylate cyclase with synthesis of cAMP. (2) APC-expressed CD80/CD86 ligands activate T cell CD28 receptors (signal 2) promoting catabolism of cAMP to signaling inert AMP, through PDE4. PDE inhibitors such as PTX, counteract cAMP degradation allowing accumulation of cAMP. cAMP activates PKA, which in turn activates CREB. CREB translocates to the nucleus and associates with CREs in gene promoters, inducing transcription of target genes including *Wnt-10b*. (3) Wnt-10b protein binds to LRP5/6 receptors leading to osteoblastogenesis/osteoblast activation and driving bone formation. (4) Direct effects of PDE-inhibitor on osteoclasts and/or osteoblasts, induce resorption, causing a high bone turnover state, but with net gain of bone mass in the axial skeleton. (B) Under immunodeficient conditions the catabolic effects of PDE dominate, leading to bone loss. APC = antigen presenting cell; CRE = CREB responsive element; CREB = cAMP responsive element binding protein; LRP5/6 = low-density lipoprotein receptor-related protein 5/6; PDE4 = phosphodiesterase-4; PKA = protein kinase A; TCR = T cell receptor.

vehicle controls. This is likely a limitation of the adoptive transfer technique in which the number and distribution of reconstituted T cells do not reach WT levels due to contraction of the T cell niche in immunodeficient animals and hence available space to accommodate T cells is diminished.<sup>(45)</sup> The anabolic response may thus have been sufficient to blunt bone loss, but inadequate to promote excess bone gain.

As with PTX, PTH also promotes bone formation in part, by eliciting Wnt-10b production by T cells, although the signaling mechanisms involved are indirect and act through promotion of regulatory T cells (Tregs), which lead to the rebalancing of nuclear factor of activated T-cells (NFAT) and suppressor of mothers against decapentaplegic (SMAD) transcription factors at the *Wnt-10b* promoter.<sup>(11)</sup> In the case of PTX, cAMP induces PKA, leading to activation of CREB, driving *Wnt-10b* promoter activity. This was evidenced by pharmacological ablation of PKA and CREB in reporter assays which abrogated cAMP-induced *Wnt-10b* expression and *Wnt-10b* promoter activation.

Based on our data, we propose a model (Fig. 5) to explain the bone anabolic actions of the PDE inhibitor PTX. In the immunosufficient state (Fig. 5A), APC bearing antigen activates the TCR and the associated CD3 complex. CD3 activation leads to induction of adenylate cyclase causing synthesis of cAMP from adenosine triphosphate (ATP). Co-stimulation through CD28 activates

PDE4, promoting catabolism of the active signaling molecule cAMP, to the signaling inert AMP, driving T cell activation and effector function. Blocking cAMP catabolism by inhibiting PDE with PTX counteracts PDE-induced cAMP removal and promotes accumulation of cAMP. cAMP stimulates activation of PKA and phosphorylation and activation of CREB. CREB translocates to the nucleus and binds to CRE within target genes involved in T cell energy including *Il-2*, but also of *Wnt-10b*. Wnt-10b secreted by CD8<sup>+</sup> T cells binds to low-density lipoprotein receptor-related protein 5/6 (LRP5/6) receptors on bone marrow stromal cells (BMSCs) and/or osteoblasts, leading to osteoblastic differentiation and/or activation of existing osteoblasts, causing bone synthesis. The direct effect of PTX on osteoblasts may lead to expression of RANKL that drives a competing bone catabolic event, causing an increase in bone resorption and development of a high bone turnover state. By contrast, under immunodeficient conditions (Fig. 5B) the direct catabolic effects of PDE on bone cells dominate, leading to bone loss.

Although TCR $\beta$  KO mice are an experimental animal model, immunocompromised human populations do exist, including HIV-infected subjects and patients receiving chemotherapeutic drugs, and subjects receiving immunosuppressive therapies to counteract transplant rejection, or for other inflammatory diseases, may be at risk of bone loss associated with PDE-based therapies.

In conclusion, our studies demonstrate that CD8<sup>+</sup> T cells are required for PDE-induced bone anabolism and involve activation of *Wnt-10b* gene transcription, induced by the cAMP signal transduction pathway.

Selective targeting of CD8<sup>+</sup> T cells with PDE inhibitors, to maximally promote bone anabolism, while minimizing the stimulatory effects of PDE inhibition on bone resorption, may constitute a novel therapeutic approach to rejuvenate bone and delay fracture in multiple osteoporotic conditions.

## Acknowledgments

Research reported in this publication was supported by grant 5I01BX000105 from the Biomedical Laboratory Research & Development Service of the VA Office of Research and Development. MNW was also supported in part, by National Institutes of Health (NIH) grants from NIAMS (AR68157, AR070091 and AR079298), and NIA (AG062334). RP was supported by NIH grants DK112946, DK119229, DK124821, and RR028009. The contents of this manuscript do not represent the views of the Department of Veterans Affairs, the NIH, or the United States Government. Histomorphometry services were performed by the University of Alabama at Birmingham, Center for Metabolic Bone Disease-Histomorphometry and Molecular Analysis Core Laboratory, supported by NIAMS (P30AR46031).

## Author contributions

**Susanne Roser-Page:** Formal analysis; investigation; methodology; writing – review and editing. **Daiana Weiss:** Formal analysis; investigation; methodology; writing – review and editing. **Tatyana Vikulina:** Formal analysis; investigation; methodology; writing – review and editing. **Mingcan Yu:** Formal analysis; investigation; methodology; writing – review and editing. **Roberto Pacifici:** Resources; writing – review and editing. **M. Neale Weitzmann:** Conceptualization; formal analysis; funding acquisition; project administration; supervision; writing – original draft; writing – review and editing.

## Conflicts of Interest Statement

All authors declare that they have no conflicts of interest.

## Peer review

The peer review history for this article is available at <https://publons.com/publon/10.1002/jbm4.10636>.

## Data Availability Statement

The data that support the findings of this study are available from the corresponding author upon reasonable request.

## References

1. Weitzmann MN, Oforokun I. Physiological and pathophysiological bone turnover—role of the immune system. *Nat Rev Endocrinol*. 2016;12(9):518-532.
2. Weitzmann MN, Pacifici R. Estrogen deficiency and bone loss: an inflammatory tale. *J Clin Invest*. 2006;116(5):1186-1194.
3. Weitzmann MN. T-cells and B-cells in osteoporosis. *Curr Opin Endocrinol Diabetes Obes*. 2014;21(6):461-467.
4. Cenci S, Weitzmann MN, Roggia C, et al. Estrogen deficiency induces bone loss by enhancing T-cell production of TNF-alpha. *J Clin Invest*. 2000;106(10):1229-1237.
5. Li JY, D'Amelio P, Robinson J, et al. IL-17A is increased in humans with primary hyperparathyroidism and mediates PTH-induced bone loss in mice. *Cell Metab*. 2015;22(5):799-810.
6. Cline-Smith A, Axelbaum A, Shashkova E, et al. Ovariectomy activates chronic low-grade inflammation mediated by memory T cells, which promotes osteoporosis in mice. *J Bone Miner Res*. 2020;35(6):1174-1187.
7. John V, Hock JM, Short LL, Glasebrook AL, Galvin RJ. A role for CD8+ T lymphocytes in osteoclast differentiation in vitro. *Endocrinology*. 1996;137(6):2457-2463.
8. Choi Y, Woo KM, Ko SH, et al. Osteoclastogenesis is enhanced by activated B cells but suppressed by activated CD8(+) T cells. *Eur J Immunol*. 2001;31(7):2179-2188.
9. Buchwald ZS, Yang C, Nellore S, et al. A bone anabolic effect of RANKL in a murine model of osteoporosis mediated through FoxP3+ CD8 T cells. *J Bone Miner Res*. 2015;30(8):1508-1522.
10. Buchwald ZS, Kiesel JR, Yang C, DiPaolo R, Novack DV, Aurora R. Osteoclast-induced Foxp3+ CD8 T-cells limit bone loss in mice. *Bone*. 2013;56(1):163-173.
11. Yu M, D'Amelio P, Tyagi AM, et al. Regulatory T cells are expanded by Teriparatide treatment in humans and mediate intermittent PTH-induced bone anabolism in mice. *EMBO Rep*. 2018;19(1):156-171.
12. Terauchi M, Li JY, Bedi B, et al. T lymphocytes amplify the anabolic activity of parathyroid hormone through Wnt10b signaling. *Cell Metab*. 2009;10(3):229-240.
13. Li JY, Yu M, Pal S, et al. Parathyroid hormone-dependent bone formation requires butyrate production by intestinal microbiota. *J Clin Invest*. 2020;130(4):1767-1781.
14. Weitzmann MN, Pacifici R. Parathyroid diseases and T cells. *Curr Osteoporos Rep*. 2017;15(3):135-141.
15. Wolf M, Lossdorfer S, Marciniak J, et al. CD8+ T cells mediate the regenerative PTH effect in hPDL cells via Wnt10b signaling. *Innate Immun*. 2016;22(8):674-681.
16. Bedi B, Li JY, Grassi F, Tawfeek H, Weitzmann MN, Pacifici R. Inhibition of antigen presentation and T cell costimulation blocks PTH-induced bone loss. *Ann N Y Acad Sci*. 2010;1192(1):215-221.
17. Axmann R, Herman S, Zaiss M, et al. CTLA-4 directly inhibits osteoclast formation. *Ann Rheum Dis*. 2008;67(11):1603-1609.
18. Roser-Page S, Vikulina T, Zayzafoon M, Weitzmann MN. CTLA-4lg-induced T cell anergy promotes Wnt-10b production and bone formation in a mouse model. *Arthritis Rheumatol*. 2014;66(4):990-999.
19. Roser-Page S, Vikulina T, Weiss D, et al. CTLA-4lg (abatacept) balances bone anabolic effects of T cells and Wnt-10b with antianabolic effects of osteoblastic sclerostin. *Ann N Y Acad Sci*. 2018;1415(1):21-33.
20. Roser-Page S, Vikulina T, Yu K, McGee-Lawrence ME, Weitzmann MN. Neutralization of CD40 ligand costimulation promotes bone formation and accretion of vertebral bone mass in mice. *Rheumatology (Oxford)*. 2018;57(6):1105-1114.
21. Wehbi VL, Tasken K. Molecular mechanisms for cAMP-mediated immunoregulation in T cells—role of anchored protein kinase signaling units. *Front Immunol*. 2016;7:222.
22. Abrahamsen H, Baillie G, Ngai J, et al. TCR- and CD28-mediated recruitment of phosphodiesterase 4 to lipid rafts potentiates TCR signaling. *J Immunol*. 2004;173(8):4847-4858.
23. Bjorgo E, Solheim SA, Abrahamsen H, et al. Cross talk between phosphatidylinositol 3-kinase and cyclic AMP (cAMP)-protein kinase signaling pathways at the level of a protein kinase B/beta-arrestin/cAMP phosphodiesterase 4 complex. *Mol Cell Biol*. 2010;30(7):1660-1672.
24. Bjorgo E, Tasken K. Novel mechanism of signaling by CD28. *Immunol Lett*. 2010;129(1):1-6.
25. Klein M, Vaeth M, Scheel T, et al. Repression of cyclic adenosine monophosphate upregulation disarms and expands human regulatory T cells. *J Immunol*. 2012;188(3):1091-1097.
26. Powell JD, Lerner CG, Ewoldt GR, Schwartz RH. The -180 site of the IL-2 promoter is the target of CREB/CREM binding in T cell anergy. *J Immunol*. 1999;163(12):6631-6639.

27. Fox KE, Colton LA, Erickson PF, et al. Regulation of cyclin D1 and Wnt10b gene expression by cAMP-responsive element-binding protein during early adipogenesis involves differential promoter methylation. *J Biol Chem*. 2008;283(50):35096-35105.
28. Kinoshita T, Kobayashi S, Ebara S, et al. Phosphodiesterase inhibitors, pentoxifylline and rolipram, increase bone mass mainly by promoting bone formation in normal mice. *Bone*. 2000;27(6):811-817.
29. Pal S, Porwal K, Singh H, et al. Reversal of osteopenia in ovariectomized rats by pentoxifylline: evidence of osteogenic and osteoangiogenic roles of the drug. *Calcif Tissue Int*. 2019;105(3):294-307.
30. Pal S, Porwal K, Khanna K, et al. Oral dosing of pentoxifylline, a pan-phosphodiesterase inhibitor restores bone mass and quality in osteopenic rabbits by an osteogenic mechanism: a comparative study with human parathyroid hormone. *Bone*. 2019;123:28-38.
31. Nguyen TTH, Eo MY, Seo MH, Myoung H, Kim SM, Lee JH. Effects of pentoxifylline and tocopherol on a rat-irradiated jaw model using micro-CT cortical bone analysis. *Eur Arch Otorhinolaryngol*. 2019;276(12):3443-3452.
32. Cakmak G, Sahin MS, Ozdemir BH, Karadeniz E. Effect of pentoxifylline on healing of segmental bone defects and angiogenesis. *Acta Orthop Traumatol Turc*. 2015;49(6):676-682.
33. Li Y, Li A, Strait K, Zhang H, Nanes MS, Weitzmann MN. Endogenous TNF $\alpha$  lowers maximum peak bone mass and inhibits osteoblastic Smad activation through NF-kappaB. *J Bone Miner Res*. 2007;22(5):646-655.
34. Degboe Y, Sunzini F, Sood S, et al. Apremilast inhibits inflammatory osteoclastogenesis. *Rheumatology (Oxford)*. 2021;61(1):452-461.
35. Vertino AM, Taylor-Jones JM, Longo KA, et al. Wnt10b deficiency promotes coexpression of myogenic and adipogenic programs in myoblasts. *Mol Biol Cell*. 2005;16(4):2039-2048.
36. Schmidt-Nielsen K. Scaling in biology: the consequences of size. *J Exp Zool*. 1975;194(1):287-307.
37. Li JY, Adams J, Calvi LM, et al. PTH expands short-term murine hemopoietic stem cells through T cells. *Blood*. 2012;120(22):4352-4362.
38. Li JY, Adams J, Calvi LM, Lane TF, Weitzmann MN, Pacifici R. Ovariectomy expands murine short-term hemopoietic stem cell function through T cell expressed CD40L and Wnt10B. *Blood*. 2013;122(14):2346-2357.
39. Li JY, Walker LD, Tyagi AM, Adams J, Weitzmann MN, Pacifici R. The sclerostin-independent bone anabolic activity of intermittent PTH treatment is mediated by T-cell-produced Wnt10b. *J Bone Miner Res*. 2014;29(1):43-54.
40. Tyagi AM, Yu M, Darby TM, et al. The microbial metabolite butyrate stimulates bone formation via T regulatory cell-mediated regulation of WNT10B expression. *Immunity*. 2018;49(6):1116-1131.e7.
41. Bouxsein ML, Boyd SK, Christiansen BA, Guldberg RE, Jepsen KJ, Muller R. Guidelines for assessment of bone microstructure in rodents using micro-computed tomography. *J Bone Miner Res*. 2010;25(7):1468-1486.
42. Kim N, Kadono Y, Takami M, et al. Osteoclast differentiation independent of the TRANCE-RANK-TRAF6 axis. *J Exp Med*. 2005;202(5):589-595.
43. Neer RM, Arnaud CD, Zanchetta JR, et al. Effect of parathyroid hormone (1-34) on fractures and bone mineral density in postmenopausal women with osteoporosis. *N Engl J Med*. 2001;344(19):1434-1441.
44. Geerman S, Hickson S, Brassier G, Pascutti MF, Nolte MA. Quantitative and qualitative analysis of bone marrow CD8(+) T cells from different bones uncovers a major contribution of the bone marrow in the vertebrae. *Front Immunol*. 2015;6:660.
45. Ofotokun I, Titanji K, Vikulina T, et al. Role of T-cell reconstitution in HIV-1 antiretroviral therapy-induced bone loss. *Nat Commun*. 2015;6:8282.